

## Influence of Diblock Addition on Tack in a Polyacrylic Triblock Copolymer/Tackifier System Measured Using a Probe Tack Test

Kazuhiro Yamamura,<sup>1</sup> Syuji Fujii,<sup>1</sup> Yoshinobu Nakamura,<sup>1</sup> Kazuko Fujiwara,<sup>2</sup> Shigeki Hikasa,<sup>3</sup> Yoshiaki Urahama<sup>3</sup>

<sup>1</sup>Department of Applied Chemistry, Osaka Institute of Technology, 5-16-1 Ohmiya, Asahi-ku, Osaka 535-8585, Japan

<sup>2</sup>Industrial Technology Center of Okayama Prefecture, 5301 Haga, Kita-ku, Okayama 701-1296, Japan

<sup>3</sup>Visiting Professor, Graduate School of University of Hyogo, 2167 Shosha, Himeji, Hyogo 671-2201, Japan

Correspondence to: Y. Nakamura (E-mail: nakamura@chem.oit.ac.jp)

**ABSTRACT:** The influence of diblock copolymer addition on the tack properties of a polyacrylic triblock copolymer/tackifier system was investigated. For this purpose, poly(methyl methacrylate)-*block*-poly(*n*-butyl acrylate)-*block*-poly(methyl methacrylate) triblock copolymer (MAM) and a 1/1 blend with a diblock copolymer consisting of the same components (MA) were used as base polymers, and a tackifier was added in amounts ranging from 10 to 30 wt %. The temperature dependence of tack was measured by a probe tack test. The tack of MAM/MA at room temperature was significantly higher than that of MAM, and the improvement of MAM/MA upon the addition of the tackifier was higher than that of MAM. The peeling process at the probe/adhesive interface during the probe tack test was observed using a high-speed microscope. It was found that for MAM/MA, cavitation was caused in the entire adhesive layer, and peeling initiation was delayed by the absorption of strain energy due to deformation of the adhesive layer. In contrast, for MAM, peeling progressed linearly from the edge to the center of the probe. The greater flexibility of the soft block chain in the diblock copolymer resulted in improved interfacial adhesion. <sup>1</sup>H pulse nuclear magnetic resonance analysis showed that the addition of the tackifier improved the cohesive strength of the adhesive. Adhesion strength is affected by two factors: the development of interfacial adhesion and cohesive strength. In the MAM/MA/tackifier system, the presence of MA and the tackifier improved the interfacial adhesion and cohesive strength, respectively. © 2012 Wiley Periodicals, Inc. *J. Appl. Polym. Sci.* 129: 1008–1018, 2013

**KEYWORDS:** adhesives; copolymers; elastomers; surfaces and interfaces

Received 15 August 2012; accepted 20 October 2012; published online 22 November 2012

DOI: 10.1002/app.38772

### INTRODUCTION

Pressure-sensitive adhesives (PSAs) typically contain a tackifier and a base polymer such as natural rubber, synthetic rubber or a block copolymer. The tackifier improves the mobility of the base polymer during the taping process by acting as a diluent and also improves the peel strength during the peeling process. Many researchers<sup>1–8</sup> have investigated the mechanism of tack improvement through the addition of tackifiers.

We are currently investigating the role of tackifiers from the viewpoint of phase structure.<sup>9–17</sup> Previously,<sup>11</sup> the effect of tackifier compatibility on the phase structure and adhesion properties of PSAs was investigated. For this purpose, a polyacrylic block copolymer consisting of poly(methyl methacrylate) (PMMA) and poly(*n*-butyl acrylate) (PBA) blocks, along with three types of tackifiers with different chemical structures and compatibilities with the polyacrylic block copolymer, were used. Agglomerates of the tackifiers were observed by

transmission electron microscopy (TEM); their sizes were found to increase from several tens of nanometers to micrometers depending on their compatibility with the base polymer. Improved adhesion properties were obtained in the phase structure when the agglomerates were of the order of several tens of nanometers.

We controlled the number of tackifier agglomerates by changing the molecular weight of a special rosin ester resin tackifier.<sup>17</sup> TEM observations showed that the number of agglomerates with a size of several tens of nanometers increased as the tackifier content and molecular weight were increased. The glass transition temperature ( $T_g$ ) of the PSA, measured by dynamic mechanical analysis, and tack, measured using a rolling cylinder tack tester, increased as the number of tackifier agglomerates increased. Based on these results, we proposed the following role for the tackifier in tack improvement: the tackifier dissolved in the base polymer improves interfacial wettability by acting as

**Table I.** Weight Average Molecular Weights, PMMA Block Contents and Polydispersities of Polyacrylic Block Copolymers Used in This Study

	$M_w^a$	PMMA block	
		content/wt%	Polydispersity <sup>b</sup>
MAM-23	78,400	23.1	1.08
MAM-16	143,800	15.9	1.11
MA	70,000	6.6	1.21

<sup>a</sup>Weight average molecular weight. <sup>b</sup> $M_w/M_n$ ,  $M_n$ : number average molecular weight.

a plasticizer, while the tackifier agglomerates, acting as filler, increase the cohesive strength of the PSA.

In general, the base block copolymer of a PSA is a blend of triblock and diblock copolymers. Pure triblock copolymers are too hard, and show lower interfacial adhesion even with a tackifier, because the molecular mobility of the soft unit in the triblock is strongly restricted by the neighboring hard units. The soft unit of diblock copolymers has a higher degree of freedom than that of triblock copolymers. However, this point has not been fully investigated until now. We also used a PMMA-*block*-PBA-*block*-PMMA triblock copolymer (MAM) and PMMA-*block*-PBA diblock copolymer (MA) blend as a base polymer for the above-mentioned studies.<sup>11,17</sup>

In this study, the adhesion properties and peeling mechanism of a MAM/MA/tackifier system were investigated and compared with the results obtained for a MAM/tackifier system to clarify the effect of MA addition. For this purpose, tack was measured using a probe tack tester at various temperatures. The peeling

process was observed during the probe tack test using a high-speed microscope. Spin-spin relaxation ( $T_2$ ) time was measured by <sup>1</sup>H pulse nuclear magnetic resonance analysis (pulse NMR), which shows the molecular mobility of PBA influenced by both the tackifier and MA.

## EXPERIMENTAL

### Materials

The weight average molecular weights ( $M_w$ ), PMMA block contents and polydispersities of MAM and MA used in this study are listed in Table I. These polyacrylic block copolymers were supplied by Kuraray Co., Ltd. (Tokyo, Japan). MAM-23 and MAM-16 were obtained in pellet form; MAM-16 is softer than MAM-23. MA is a viscous liquid. A special rosin ester resin with a softening point of 108–120°C,  $M_w$  of 890, polydispersity of 1.2 and  $T_g$  of 70°C (SE-A-115, Arakawa Chemical Industries, Ltd., Osaka, Japan) was used as a tackifier. Chemical structures of tackifier are shown in Figure 1. The used tackifier is mixture of a, b and c. Reagent-grade toluene was used.

### Sample Preparation

Solutions of 50 wt % base polymer/tackifier in toluene were prepared. The tackifier content in the solid ranged from 10 to 30 wt %. The solutions were cast on a polyethylene terephthalate (PET, thickness: 38  $\mu$ m) sheet. After evaporation of the toluene at room temperature, the cast film was heated at 100°C for 10 min in a vacuum. The thickness of the resulting PSA layer was measured using a thickness indicator (Dial thickness gauge H-MT, Ozaki, Tokyo, Japan) and was typically determined to be about 50  $\mu$ m.

To prepare thick sheet specimens for dynamic viscoelastic measurement, toluene solutions were cast onto a release paper and

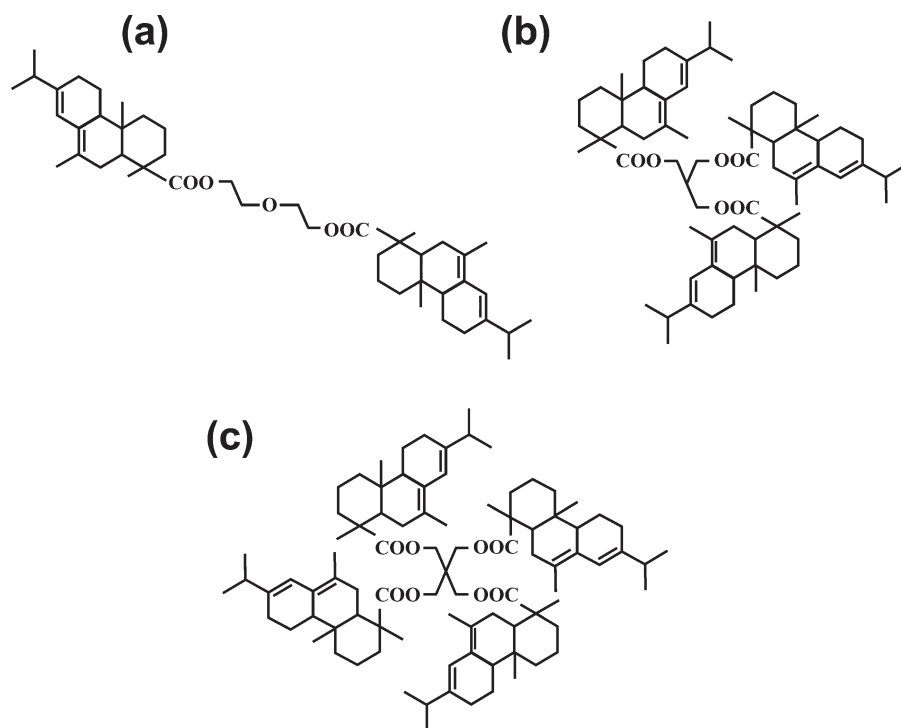


**Figure 1.** Structures of tackifier used.

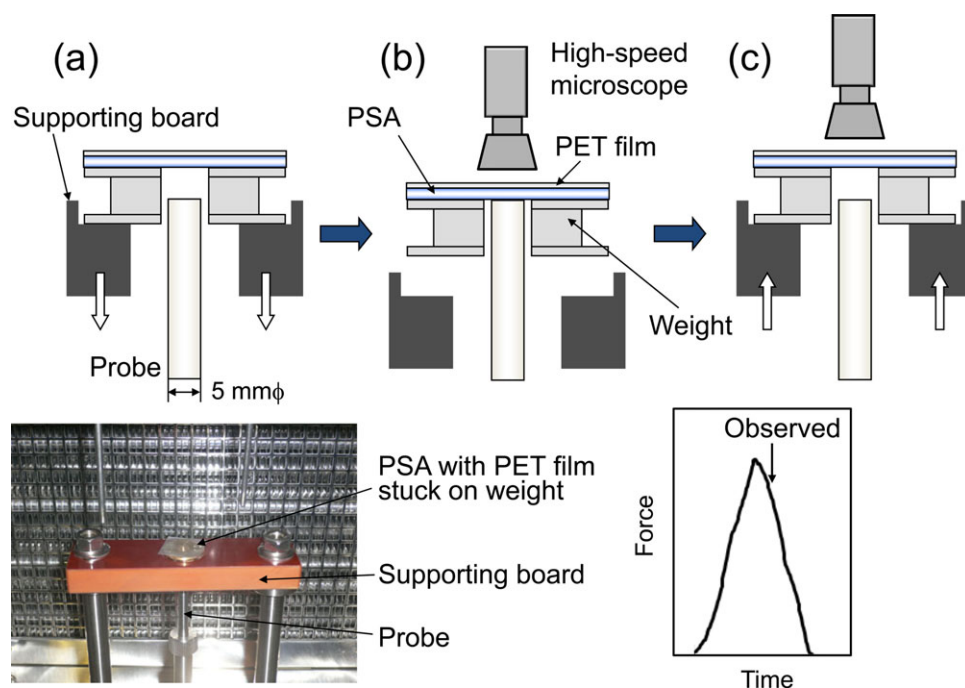


**Figure 2.** Schematic of the test procedure and measurement component of the probe tack tester. The arrow mark in the force-time curve indicates the observation point for the static high-speed microscope images shown in Figures 8–10. [Color figure can be viewed in the online issue, which is available at [wileyonlinelibrary.com](http://wileyonlinelibrary.com).]

toluene was evaporated at room temperature for 1 week. The thickness of these thick sheet samples was about 2 mm.

### TEM Observation

TEM images were obtained with a TEM (H7100FA, Hitachi, Ltd., Tokyo, Japan) using an acceleration voltage of 100 kV. The PSA was sliced into thin sections of about 80 nm thickness using a low-temperature ultramicrotome (Ultracut S/FCS, Leica Microsystems, Wetzlar, Germany) after freezing in liquid nitrogen. The thin sections were stained with vapors of an aqueous 0.5% RuO<sub>4</sub> solution for 3 min or by dipping in 10–15% phosphorous tungstate aqueous (PTA) solution.<sup>18</sup>

### Tack

Tack was measured using a probe tack tester (TE-6002, Tester Sangyo Co., Ltd., Saitama, Japan) with a probe 5 mm in diameter, made of stainless steel, in the temperature range from 0 to 80°C.<sup>16</sup> A schematic of the test procedure and the measurement component of the probe tack tester are shown in Figure 1. PSA tapes are attached to a weight, which is set on a supporting board (a). When the tack measurement is started, the supporting board descends. When the probe thrusts up the weight, contact between the probe and the sample adhesive tape begins (b). After a set contact time, the supporting board begins to elevate. Peeling takes place at this time (c). The force-time curve during the peeling process was recorded, and the tack value was calculated from the maximum stress value in the curve. The compression force of the weight was 0.10 N and the contact time was set at 30 s. The displacement rate of the supporting board was 10 mm/s. In this probe tack tester, the probe was fixed and the supporting board moved up and down. For

convenience, the displacement rate of the supporting board is hereafter denoted as the apparent probe velocity.

The top view of the adhesive during the peeling process was observed using a high-speed microscope (VW-6000, Keyence Corp., Osaka, Japan) at room temperature (23–25°C). A typical force-time curve measured from the probe tack test is also shown in Figure 2. The arrow in the schematic force-time curve indicates the observation point for the static high-speed microscope images shown in Figures 8–10.

### Peel Strength

The PSA tapes prepared as described above was cut in strips of 25 mm width and then the strip was placed onto a stainless steel plate (SUS304BA, Nippon Tact Co. Ltd., Tokyo, Japan) used as an adherend. The strip on the stainless steel was pressed using a 2-kg iron roller to develop good contact between the adhesive and the steel plate. Test specimens were subjected to five press cycles: the iron roller moved backward and forward as one press cycle. Some test specimens were further heated in the range from 40°C to 120°C for 2 h after five press cycles to improve the interfacial adhesion. The peel test was conducted 20–40 min after specimen preparation.

The 180° peel strength was measured at a peel rate of 300 mm/min at room temperature (23–25°C) using a tensile testing machine (AG-5KNIS, Shimadzu Corp., Kyoto, Japan) in accordance with JIS Z 0237 (Japanese Industrial Standards) in the same way as in the previous studies.<sup>9–14</sup>

### Dynamic Viscoelastic Properties

The 2-mm-thick sheets prepared as described above were cut into rectangles (9 mm × 40 mm) and peeled off. The

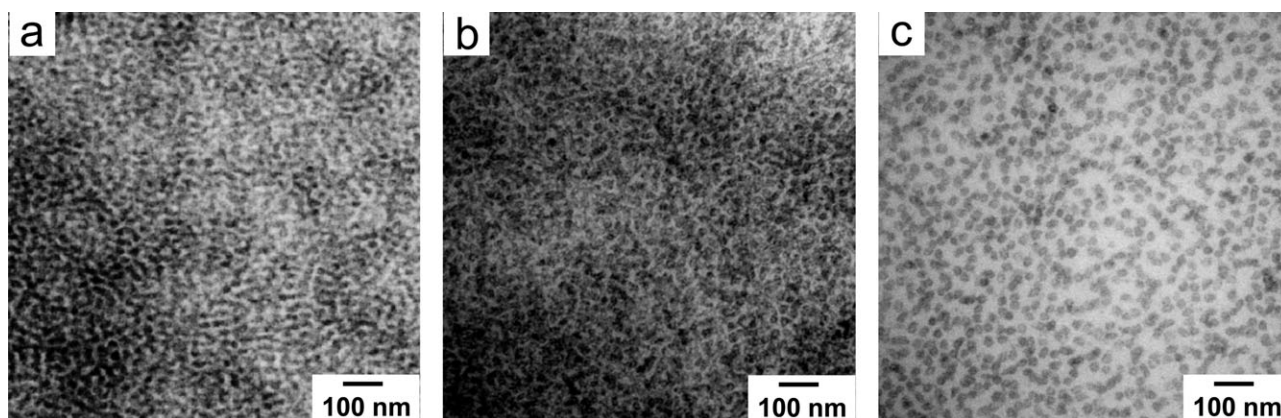


**Figure 3.** TEM images of thin sections of MAM-23 (a), MAM-23/MA (1/1, w/w) (b) and MAM-16 (c). TEM samples were stained with PTA.

temperature dependence of the dynamic viscoelastic properties was studied using a dynamic mechanical analyzer (DMS-6000, SII NanoTechnology Inc., Chiba, Japan) in tensile mode at a frequency of 10 Hz as reported previously.<sup>17</sup>

### Molecular Mobility

In order to evaluate molecular mobility within the adhesives, pulse NMR measurements (JNM-MU25, resonance frequency of 25 MHz, JEOL Ltd., Tokyo, Japan) were carried out using the solid echo method at 20°C and 60°C as previously reported.<sup>9–11,13,14,16</sup> In these experiments, the sampling time was 2 ms, the integration was carried out 128 times, the pulse width of the radiofrequency wave was 2.2  $\mu$ s, the pulse interval was 8.0  $\mu$ s and the repeat time of the pulse wave was 4.0 s.

The obtained free induction decay (FID) curves were analyzed as follows in accordance with the method proposed by Urahama<sup>19</sup>: the FID amplitude (the signal intensity at 0 ms) was normalized—i.e., the FID curves were corrected to make the FID amplitude constant—and then the normalized FID curves were differentiated. The time axis of the analyzed result is shown logarithmically. However, when the data measured with a fixed time interval are shown logarithmically, the data points become sparse in the shorter relaxation time region. Unfortunately, the number of points that can be obtained in one measurement using this apparatus is limited to 2000. For this reason, we measured four times with different measuring ranges of 400, 1000, 4000, and 8000  $\mu$ s, and the four results were put together.

## RESULTS AND DISCUSSION

For the purpose of this study, it is desirable to use MAM and MA with the same PMMA block content. Regrettably, the PMMA block contents in MAM-23 and MA were different (23.1 and 6.6 wt %, respectively), as shown in Table I; therefore, the PMMA content of MAM-23/MA (1/1, w/w) was 14.9 wt %. In order to clarify the influence of PMMA content, MAM-16 with a PMMA content similar to that of MAM-23/MA was used. However, it must be taken into consideration that the average molecular weight of MAM-16 is far greater than that of MAM-23.

The TEM images of base polymers stained with PTA are shown in Figure 3. PTA stains PMMA preferentially than PBA. A sea-island structure with spherical PMMA domains possessing a

mean size of about 20 nm dispersed in the PBA continuous phase was observed in all base polymers.

Figure 4 shows the TEM images of MAM-23/MA/tackifier system stained with RuO<sub>4</sub> at tackifier contents of 10 (a) and 30 wt % (b). RuO<sub>4</sub> stains tackifier preferentially. In these TEM images, the PBA continuous phase is stained gray. This indicates that the tackifier exists in the PBA continuous phase rather than in the PMMA domains. The black spots with several tens of nanometers in size are the agglomerates of tackifier as clarified in our previous reports.<sup>11,17</sup> The number of agglomerates increased with increasing tackifier content.

The temperature dependences of tack are shown in Figures 5–7. The apparent probe velocity was 10 mm/s and the contact time was 30 s. The failure mode was interfacial failure for all specimens. Figure 5 shows the result for the MAM-23/tackifier system. For pure MAM-23, tack increased with temperature, showing a maximum value at 50°C, then decreased. The addition of tackifier at 10 wt % did not improve tack to a significant extent; however, when the tackifier was added at greater than 20 wt %, tack was improved, depending on the content. The tack values of systems containing the tackifier were lower than that of pure MAM-23 at low temperatures.

Figure 6 shows the temperature dependence of tack for the MAM-16/tackifier system. The tack of pure MAM-16 was higher at 20°C or less, but lower in the range above 40°C, than that of pure MAM-23. The tack of the MAM-16/tackifier system was improved in the range of 30°C or less compared to that of the MAM-23/tackifier system.

Figure 7 shows the temperature dependence of tack for the MAM-23/MA/tackifier system. The tack of MAM-23/MA at 40°C or less was significantly higher than those of MAM-16 and MAM-23. The addition of the tackifier resulted in a dramatic improvement in tack above 30°C, and it continued to improve as the content was increased.

The tack of MAM-23/MA at room temperature was the highest among the three types of base polymers. And the tack after tackifier addition was also highest in the MAM-23/MA/tackifier system. The tack properties of this system were better than those of the MAM-16 system, although the PMMA contents were similar.

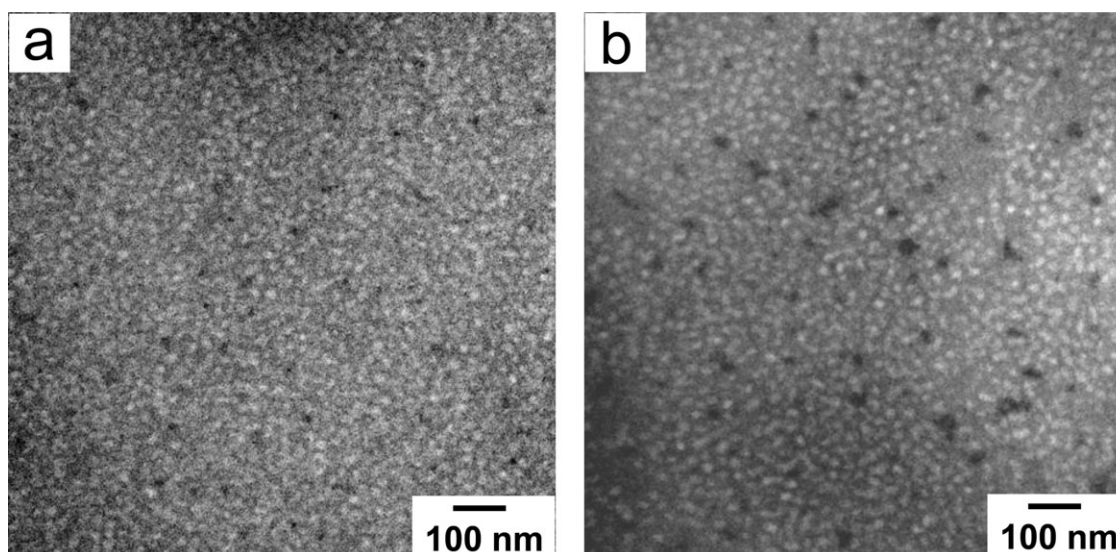


**Figure 4.** TEM images of thin sections of MAM-23/MA/tackifier system at tackifier contents of 10 (a) and 20 wt % (b). MAM-23/MA mixing ratio is 1/1 (w/w). TEM samples were stained with RuO<sub>4</sub>.

The fracture energy was also measured, based on the area surrounding the stress-displacement curve for the tack measurement; however, there was no significant difference in the tendencies of tack and fracture energy. This is because the PSAs used in this study were comparatively hard and did not cause fibrillation.

The measurement part of the probe tack tester used in this study is a temperature-controlled chamber; therefore, observation of peeling by opening the lid is possible only at room temperature. Peeling between the probe surface and the PSA was observed using a high-speed microscope at 23°C, and still pictures were chosen from the continuously recorded data. The observation point was just after the maximum value in the force-time curve shown in Figure 2.

Figure 8 shows the result for the MAM-23/tackifier system. Peeling advanced linearly from the edge of the probe toward the center. The boundary between the peeled and unpeeled parts was clearly observed. There was no difference in the peeling mechanisms with and without the tackifier.

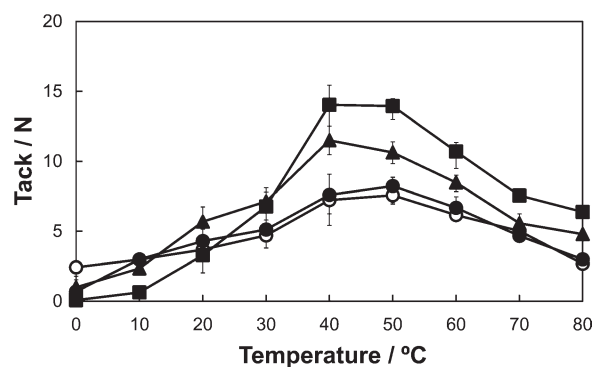
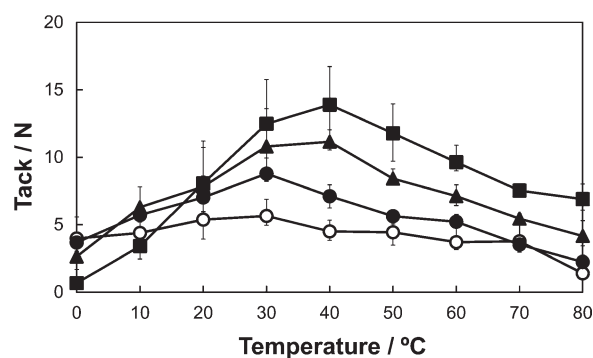


**Figure 5.** Temperature dependence of tack for the MAM-23 (○) and MAM-23/tackifier systems (●, ▲, ■) at tackifier contents of 10 (●), 20 (▲) and 30 wt % (■) measured by a probe tack test with a contact time of 30 s and apparent probe velocity of 10 mm/s.

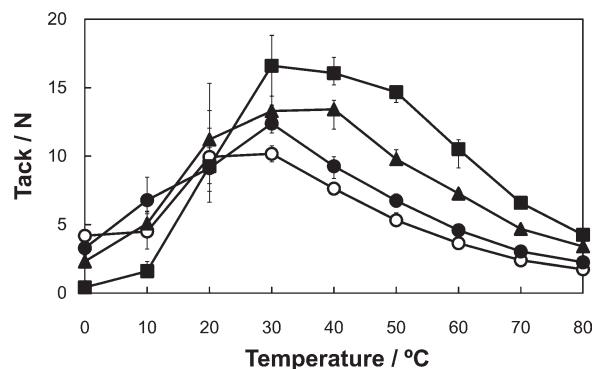
Figure 9 shows the result for the MAM-16/tackifier system. Many holes were formed at the edge of the probe, because cavitation was caused.

Figure 10 shows the result for the MAM-23/MA/tackifier system; again, many holes were formed at the edge of the probe, although no holes were observed in the system containing 30 wt % tackifier. However, the difference between the peeling mechanisms of the MAM-16 and MAM-23/MA systems was unclear from Figures 9 and 10. So, the images of peeling during probe tack test for MAM-16 and MAM-23/MA were compared in detail.

Figure 11 shows the force-time curve measured by probe tack test and the still pictures of probe tip for MAM-16 during probe tack test. The cavitation was caused at the edge of the probe with an increase of stress without interfacial peeling (a). After the maximum stress, the circular band of holes was more in the center and the area outside the band of holes was peeled out (b → c → d). That is, the cavitation was caused only at the boundary of the peeled and unpeeled areas.



**Figure 6.** Temperature dependence of tack for the MAM-16 (○) and MAM-16/tackifier systems (●, ▲, ■) at tackifier contents of 10 (●), 20 (▲) and 30 wt % (■) measured by a probe tack test with a contact time of 30 s and apparent probe velocity of 10 mm/s.



**Figure 7.** Temperature dependence of tack for the MAM-23/MA (○) and MAM-23/MA/tackifier systems (●, ▲, ■) at tackifier contents of 10 (●), 20 (▲) and 30 wt % (■) measured by a probe tack test with a contact time of 30 s and apparent probe velocity of 10 mm/s.

Figure 12 shows the force-time curve and the still pictures of probe tip for MAM-23/MA. The cavitation was caused at the edge of the probe with an increase of stress without interfacial peeling (a). This is completely the same as MAM-16 (Figure 11). After the maximum stress, the region in which the cavitation was caused was spread toward the center (b → c). However, the peeled part was not observed. This completely differed from MAM-16 (Figure 11).

On the other hand, the peeling occurred at the maximum stress, and it advanced linearly from the edge of the probe toward the center immediately for MAM-23 (The data was omitted).

The observed peeling mechanism is depicted schematically in Figure 13. For the MAM-23 system (a), peeling progressed linearly from the edge to the center of the probe after the maximum stress. For the MAM-16 system (b), the cavitation was caused at the peeling tip and deformation of the PSA layer due to hole generation inhibited the progress of peeling. The cavitation was caused in the wider region of the PSA layer delayed the initiation of peeling for the MAM-23/MA system (c). Thus,

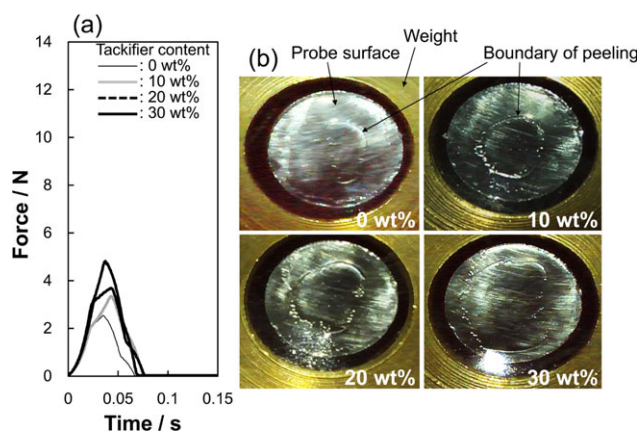


**Figure 8.** Force-time curves for the MAM-23/tackifier system measured by a probe tack test (a), and static images of the peeling process observed by a high-speed microscope (b). The observation point is indicated by the arrow mark in Figure 2. [Color figure can be viewed in the online issue, which is available at [wileyonlinelibrary.com](http://wileyonlinelibrary.com).]

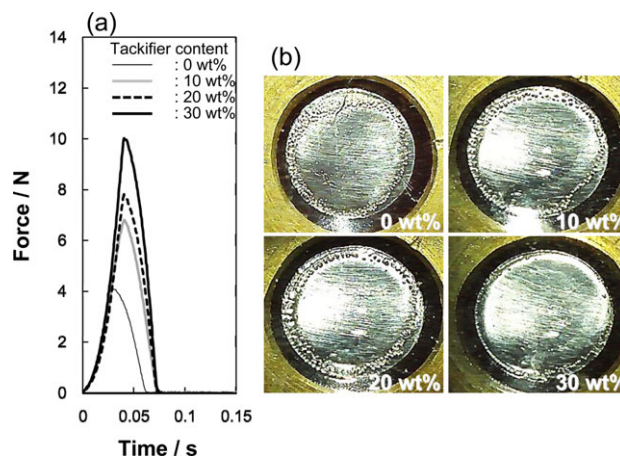


**Figure 9.** Force-time curves for the MAM-16/tackifier system measured by a probe tack test (a), and static images of the peeling process observed by a high-speed microscope (b). The observation point is indicated by the arrow mark in Figure 2. [Color figure can be viewed in the online issue, which is available at [wileyonlinelibrary.com](http://wileyonlinelibrary.com).]

in the MAM-23 system, the strain energy was absorbed by the progress of peeling, while in the MAM-16 and MAM-23/MA systems, it was absorbed by the deformation of the PSA layer. The effect was greater for the MAM-23/MA system. These results indicate that interfacial adhesion was in the order MAM-23/MA > MAM-16 > MAM-23.

As mentioned above, the PSAs used in this study were comparatively hard and did not cause fibrillation. Therefore, interfacial peeling took place the moment after the image of Figure 12(c), even in the MAM-23/MA system.

For MAM-23/MA with a tackifier content of 30 wt %, holes were never observed (Figure 10). This is because the high-concentration tackifier improved the cohesive strength of the PSA, as mentioned earlier,<sup>11,17</sup> and the deformation ability by the addition of MA decreased.

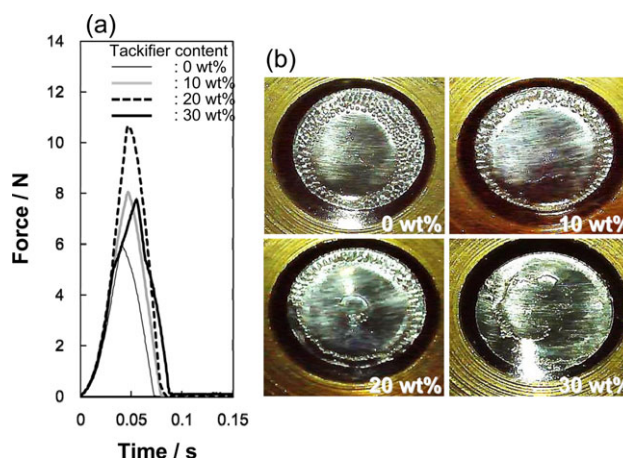


**Figure 10.** Force-time curves for the MAM-23/MA/tackifier system measured by a probe tack test (a), and static images of the peeling process observed by a high-speed microscope (b). The observation point is indicated by the arrow mark in Figure 2. [Color figure can be viewed in the online issue, which is available at [wileyonlinelibrary.com](http://wileyonlinelibrary.com).]

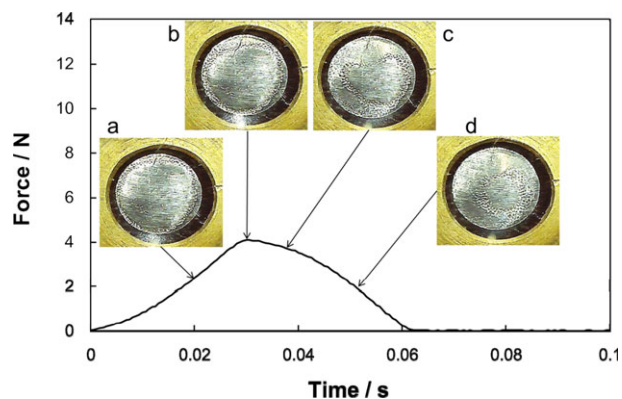


**Figure 11.** Peeling behavior observed by a high-speed microscope and force-time curve measured by a probe tack test for MAM-16 with a contact time of 30 s and apparent probe velocity of 10 mm/s. [Color figure can be viewed in the online issue, which is available at [wileyonlinelibrary.com](http://wileyonlinelibrary.com).]

Next,  $180^\circ$  peel strength was measured. In order to clarify the influence of interfacial adhesion, the test specimen was heated to a temperature in the range  $40\text{--}120^\circ\text{C}$  for 2 h before the peel test. Figure 14 shows the peel strength of the MAM-23/tackifier system; the term “As-prepared” denotes a specimen that did not undergo preheating. The peel strength of pure MAM-23 increased as the preheating temperature increased above  $50^\circ\text{C}$ , because the interfacial adhesion was improved by heating. Preheating had no influence on the improvement of peel strength in the systems containing the tackifier. The peel strengths for systems with tackifier contents of 10 and 20 wt % were almost equal to the lowest peel strength of MAM-23, whereas that of the system containing 30 wt % tackifier was equivalent to the highest value.

Previously, the role of the tackifier was investigated from the point of view of the relationship between the phase structure of model PSAs, as observed by TEM, and the adhesion properties.<sup>11,17</sup> In

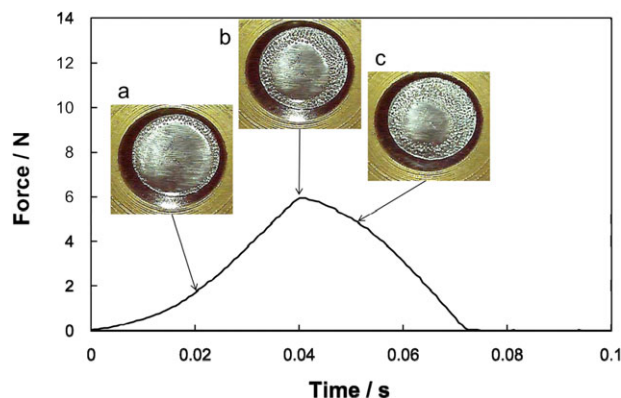
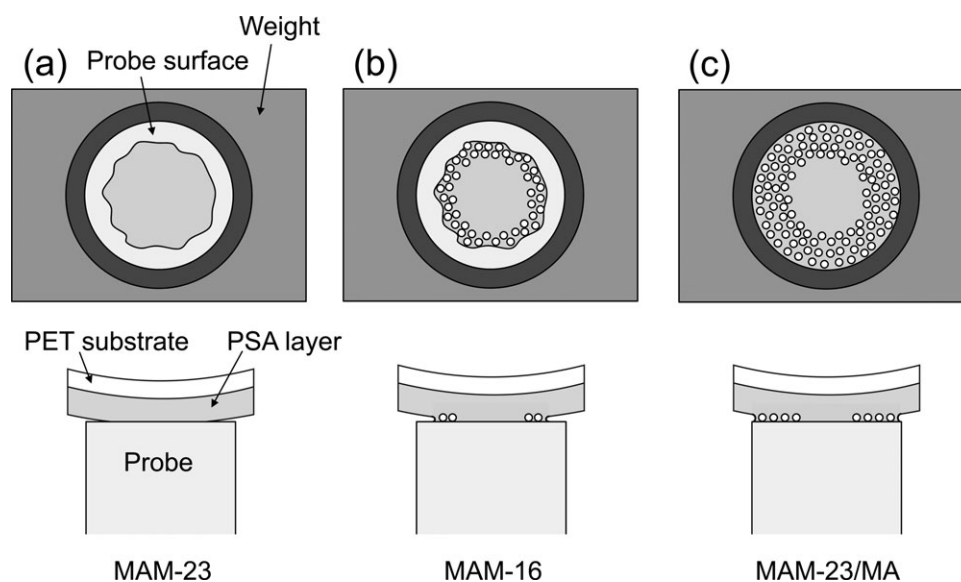


**Figure 12.** Peeling behavior observed by a high-speed microscope and force-time curve measured by a probe tack test for MAM-23/MA (1/1, w/w) with a contact time of 30 s and apparent probe velocity of 10 mm/s. [Color figure can be viewed in the online issue, which is available at [wileyonlinelibrary.com](http://wileyonlinelibrary.com).]

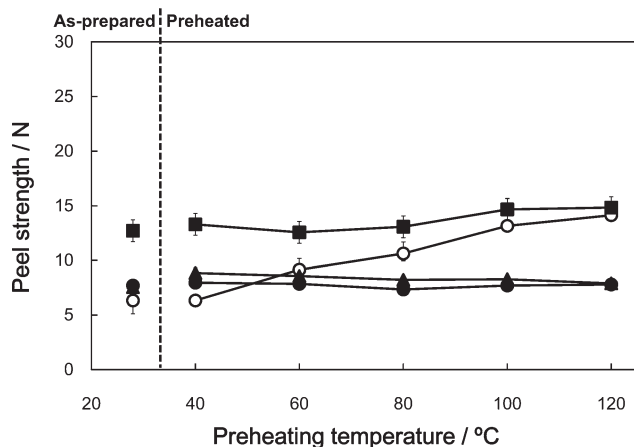
this regard, we proposed the following role for a tackifier in the development of tack: a tackifier dissolved in the base polymer improves interfacial wettability by acting as a plasticizer, while tackifier agglomerates several tens of nanometers in size act as filler to increase the cohesive strength of the adhesive. The number of agglomerates increases at higher tackifier concentrations. That is, the improving effect of cohesive strength was insufficient at tackifier contents of less than 20 wt %, but at 30 wt % it was sufficient to improve peel strength.

Figure 15 shows the peel strength of the MAM-16/tackifier system. The degree of improvement in the peel strength of pure MAM-16 with preheating was lower than that of pure MAM-23 (Figure 14).

Figure 16 shows the peel strength of the MAM-23/MA/tackifier system. The peel strength of MAM-23/MA was improved by preheating to  $40^\circ\text{C}$ ; however, there was no further improvement



**Figure 13.** Schematic top (upper) and side (lower) views of the peeling process measured by a probe tack test, for (a) MAM-23, (b) MAM-16 and (c) MAM-23/MA.



**Figure 14.** 180° peel strength for the MAM-23 (○) and MAM-23/tackifier systems (●, ▲, ■) at tackifier contents of 10 (●), 20 (▲) and 30 wt % (■). The test specimen was pressed 5 times with a 2 kg iron-roller (as-prepared) or pressed five times and then heated to 40–120°C for 2 h before the peel test (preheated). Fracture mode is interfacial failure for all specimens. The tape width is 25 mm and the peel rate is 5 mm/s.

by preheating to temperatures beyond 40°C. MAM-23/MA showed sufficient interfacial adhesion without heating to high temperatures.

Based on the results shown in Figures 14–16, the order of interfacial adhesion is as follows: MAM-23/MA > MAM-16 > MAM-23.

Preheating to 100–120°C caused the peel strength of MAM-23/MA to fall, whereas those of the tackifier-containing systems rose (Figure 16). Originally these phenomena cannot occur. Since the molecular mobility of MA is high, maldistribution and the migration of MA and tackifier molecules to the adherend interface at high temperatures, or a change in the phase structure of the tackifier, may have been responsible.

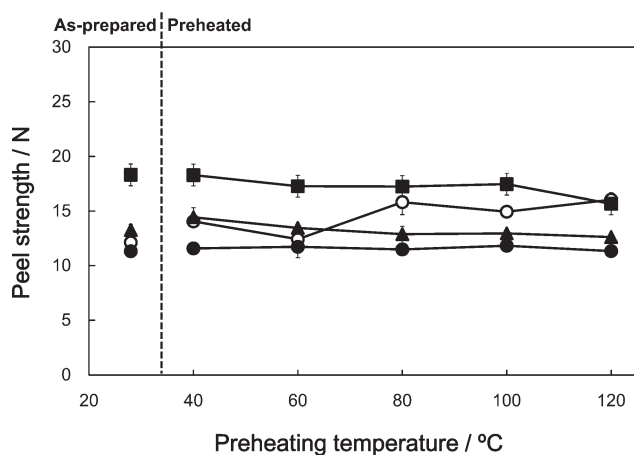


**Figure 15.** 180° peel strength for the MAM-16 (○) and MAM-16/tackifier systems (●, ▲, ■) at tackifier contents of 10 (●), 20 (▲) and 30 wt % (■). The test specimen was pressed five times with a 2 kg iron-roller (as-prepared) or pressed five times and then heated to 40–120°C for 2 h before the peel test (preheated). Fracture mode is interfacial failure for all specimens. The tape width is 25 mm and the peel rate is 5 mm/s.

The  $\tan \delta$  peak temperature (that is,  $T_g$ ) of the PBA phase, measured by dynamic mechanical analysis, was increased by the addition of the tackifier; the degree of increase was dependent on the amount of the tackifier.<sup>11,17</sup> This was influenced by the number of tackifier agglomerates tens of nanometers in size, as clarified previously.<sup>11,17</sup> As PSA is a typical viscoelastic material, its viscoelastic property follows a time-temperature superposition law<sup>20–22</sup>; that is, a low temperature is equal to a high velocity and a high temperature is equal to a low velocity. There is a strong correlation between a rise in the  $T_g$  of the PBA phase at low temperatures and resistance to peeling, namely the cohesive strength.<sup>12,17</sup>

Figure 17 shows the relationship between the  $\tan \delta$  peak temperatures and the tackifier content obtained by dynamic mechanical analysis for all of the base polymer/tackifier systems. The  $\tan \delta$  peak temperatures rose with the tackifier content. The measured  $\tan \delta$  peak temperature values were compared with the  $T_g$  values calculated by the rule of mixtures (Fox equation<sup>23</sup>) using the  $T_g$  values of the pure base polymers and the tackifier. The  $T_g$  values of the MAM-23/tackifier and MAM-23/MA/tackifier systems were the same, while that of the MAM-16/tackifier system was lower. The molecular weight of the middle PBA block of MAM-16 is very large, as shown in Table I; this may have influenced the decrease in  $T_g$ . The actual measured value became higher than that calculated by the rule of mixtures with the addition of the tackifier at 20 to 30 wt %. Tackifier agglomerates tend to be generated at higher contents and the effect of the improvement in the cohesive strength is stronger.<sup>17</sup> Based on these results, the increase in cohesive strength due to the addition of the tackifier became more significant at higher concentrations.

Pulse NMR measurements were also obtained to clarify the effect of tackifier addition on the restriction of molecular mobility in the PBA unit. For this paper, the measured FID curves were normalized and differentiated; in this way, the

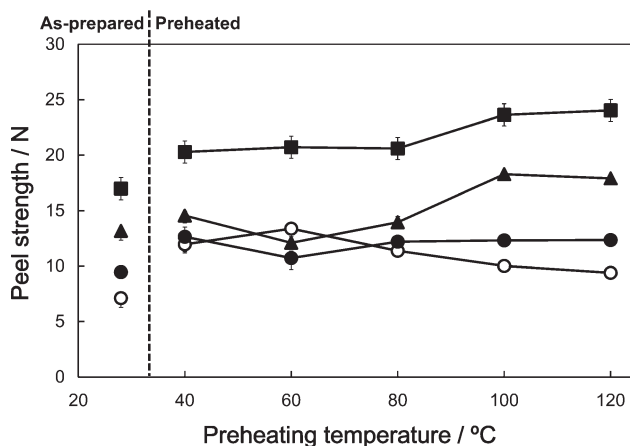


**Figure 16.** 180° peel strength for the MAM-23/MA (○) and MAM-23/MA/tackifier systems (●, ▲, ■) at tackifier contents of 10 (●), 20 (▲) and 30 wt % (■). The test specimen was pressed five times with a 2 kg iron-roller (as-prepared) or pressed five times and then heated to 40–120°C for 2 h before the peel test (preheated). Fracture mode is interfacial failure for all specimens. The tape width is 25 mm and the peel rate is 5 mm/s.



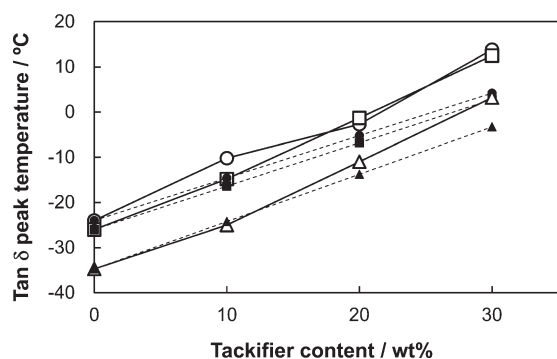


**Figure 17.**  $\tan \delta$  peak temperature for MAM-23/tackifier ( $\circ$ ), MAM-16/tackifier ( $\triangle$ ) and MAM-23/MA/tackifier ( $\square$ ) systems measured by dynamic mechanical analysis at 10 Hz in tensile mode. The closed symbols show the  $T_g$  values calculated in accordance with the rule of mixtures (Fox equation) using the  $T_g$  values of the pure base polymers and tackifier for the MAM-23/tackifier ( $\bullet$ ), MAM-16/tackifier ( $\blacktriangle$ ) and MAM-23/MA/tackifier ( $\blacksquare$ ) systems.

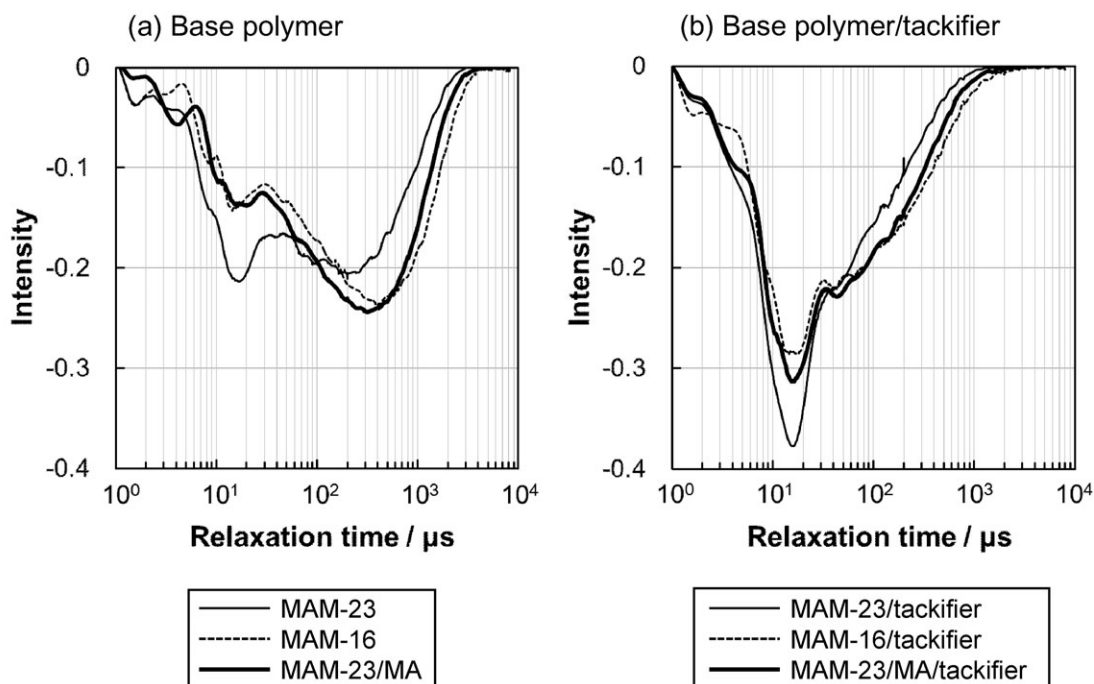
relaxation time and distribution of specific components were clearly shown. Figure 18 shows normalized and differentiated FID curves for the base polymers (a) and systems containing the tackifier (b) as measured by pulse NMR at 20°C. Measurements were also obtained for pure MA. However, MA was a viscous liquid, while the other materials were soft solids, as mentioned above. The solid echo technique used in this study is a measuring method suitable for solid samples. For this reason, the result for MA is not included in the Figure. For the base polymer [Figure 18(a)], the peak appearing between  $10^1$  and  $2 \times 10^1 \mu\text{s}$  is due to relaxation of the PMMA unit. The depth of this peak depends on the PMMA content of the base polymer

(MAM-23: 23.1 wt %, MAM-16: 15.9 wt %, MAM-23/MA: 14.9 wt %). The peak between  $2 \times 10^2$  and  $5 \times 10^2 \mu\text{s}$  is due to relaxation of the PBA unit. The relaxation time of MAM-23 was the shortest, followed by MAM-23/MA and MAM-16. It was shown that restriction of the molecular mobility of the PBA unit by the PMMA unit was in this order.

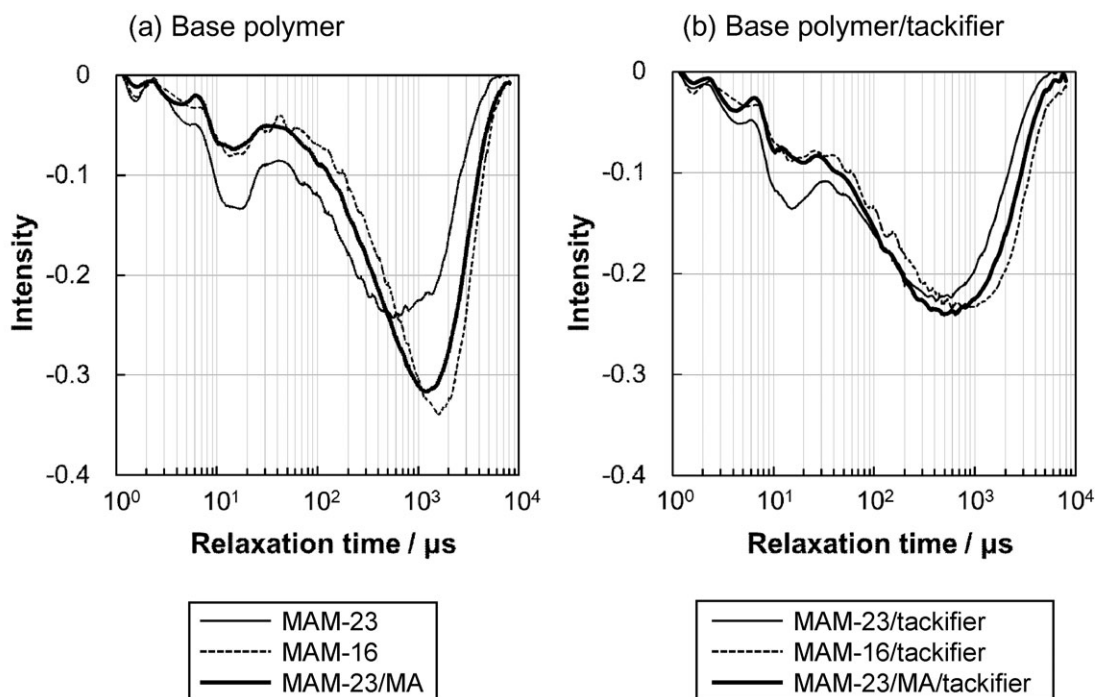
In the systems containing the tackifier [Figure 18(b)], the peak appearing between  $10^1$  and  $2 \times 10^1 \mu\text{s}$ , due to relaxation of the PMMA unit, became significantly deeper. As explained previously, tackifier agglomerates form at high concentrations.<sup>17</sup> This result indicates that their hardness is the same as that of the PMMA domain. The peak for PBA appeared between  $4 \times 10^1$  and  $5 \times 10^1 \mu\text{s}$ , becoming smaller and shifting to the region of shorter relaxation time. The tackifier agglomerates act as filler, restricting the molecular mobility of PBA, as clarified previously.<sup>11,17</sup> This causes shifting and reduction of the PBA relaxation peak.

Figure 19 shows similar results measured at 60°C. In the base polymer [Figure 19(a)], the depth of the peak between  $10^1$  and  $2 \times 10^1 \mu\text{s}$ , which is caused by relaxation of PMMA unit, decreased. The PBA peak appeared between  $4 \times 10^2$  and  $2 \times 10^3 \mu\text{s}$ , becoming larger and shifting to the region of longer relaxation time compared with the result obtained at 20°C [Figure 18(a)]. Molecular motion becomes greater at 60°C, which affects the part of the PMMA unit adjoining the PBA unit.

In the systems containing the tackifier [Figure 19(b)], the depth of the peak between  $10^1$  and  $2 \times 10^1 \mu\text{s}$ , based on the relaxation of the PMMA unit and agglomerates of tackifier, decreased significantly compared with the result obtained at 20°C [Figure 18(b)]. The PBA relaxation peak, appearing clearly between  $4 \times 10^2$  and  $10^3 \mu\text{s}$ , became far larger and shifted toward the region of longer



**Figure 18.** Normalized and differentiated FID curves for the base polymers (a) and the same systems with added tackifier (b) as measured by pulse NMR at 20°C. The MAM-23/MA mixing ratio is 1/1 (w/w) and the tackifier content is 30 wt %.



**Figure 19.** Normalized and differentiated FID curves for the base polymers (a) and the same systems with added tackifier (b) as measured by pulse NMR at 60°C. The MAM-23/MA mixing ratio is 1/1 (w/w) and the tackifier content is 30 wt %.

relaxation time. The degree of restriction of the molecular mobility of PBA by the tackifier decreased due to the increased molecular motion of PBA at 60°C. The PBA relaxation peak in the systems containing the tackifier still appeared at a shorter relaxation time than the base polymers, showing that the tackifier restricts the molecular mobility of the PBA unit even at 60°C.

Adhesive strength is affected by two factors: the development of interfacial adhesion and the cohesive strength of the adhesive.<sup>24,25</sup> As explained above, the tackifier was effective in raising the cohesive strength, and this was not dependent on the base polymer. The use of MA resulted in an improvement of interfacial adhesion. This is why the adhesion strength of MAM/MA/tackifier system was the largest among those studied.

## CONCLUSIONS

The adhesion properties of MAM-23, MAM-16, and MAM-23/MA, and the same systems with a tackifier added, were investigated and their molecular mobility was measured using pulse NMR to clarify the effect of MA addition. The following results were obtained.

1. Among the base polymers at 20–40°C, the tack values were highest for MAM-23/MA/tackifier systems, based on the temperature dependence of tack.
2. Observation of the peeling process showed that cavitation was caused throughout the PSA layer, and the initiation of peeling was delayed by the absorption of strain energy which occurred due to this deformation for MAM-23/MA containing less than 20 wt % tackifier. Peeling progressed from edge of the probe to the center and was more linearly in the MAM-23 and MAM-16 systems. The MAM-23/MA system showed higher interfacial adhesion.

3. From the rise in the  $\tan \delta$  peak temperature ( $T_g$ ), measured by dynamic mechanical analysis, and the relaxation times, measured by pulse NMR, it was concluded that the addition of the tackifier reduced the molecular mobility of PBA, namely raised the cohesive strength of PSA.
4. In the MAM-23/MA/tackifier system, MA and the tackifier were effective in improving interfacial adhesion and cohesive strength, respectively. This is the reason for the high tack and peel strength of this system.

## ACKNOWLEDGMENTS

The authors are grateful to Kuraray Co., Ltd. (Tokyo, Japan) and Arakawa Chemical Industries, Ltd. (Osaka, Japan) for their kind donations of the block polymers and tackifier, respectively.

## REFERENCES

1. Wetzel, F. H.; *Rubber Age* **1957**, *82*, 291.
2. Sherriff, M.; Knibbs, R. W.; Langley, P. C. *J. Appl. Polym. Sci.* **1973**, *17*, 3423.
3. Aubrey, D. W. *Rubber Chem. Technol.* **1988**, *61*, 448.
4. Kumar, K. D.; Gupta, S.; Tsou, A. H.; Bhowmick, A. K. *J. Appl. Polym. Sci.* **2008**, *110*, 1485.
5. Kim, J.; Han, C. D.; Chu, S. G. *J. Polym. Sci. Polym. Phys.* **1988**, *26*, 677.
6. Class, J. B.; Chu, S. G. *J. Appl. Polym. Sci.* **1985**, *30*, 805.
7. Takemoto, M.; Kajiyama, M.; Mizumachi, H.; Takemura, A.; Ono, H. *J. Appl. Polym. Sci.* **2002**, *83*, 719.
8. Basak, G. C.; Bandyopadhyay, A.; Bhowmick, A. K. *Int. J. Adhesion Adhesives* **2010**, *30*, 489.

9. Sasaki, M.; Nakamura, Y.; Fujita, K.; Kinugawa, Y.; Iida, T.; Urahama, Y. *J. Adhesion Sci. Technol.* **2005**, *19*, 1445.
10. Sasaki, M.; Fujita, K.; Adachi, M.; Fujii, S.; Nakamura, Y.; Urahama, Y. *Int. J. Adhesion Adhesives* **2008**, *28*, 372.
11. Nakamura, Y.; Sakai, Y.; Adachi, M.; Fujii, S.; Sasaki, M.; Urahama, Y. *J. Adhesion Sci. Technol.* **2008**, *22*, 1313.
12. Nakamura, Y.; Adachi, M.; Tachibana, Y.; Sakai, Y.; Nakano, S.; Fujii, S.; Sasaki, M.; Urahama, Y. *Int. J. Adhesion Adhesives* **2009**, *29*, 806.
13. Sasaki, M.; Adachi, M.; Kato, Y.; Fujii, S.; Nakamura, Y.; Urahama, Y.; Sakurai, S. *J. Appl. Polym. Sci.* **2010**, *118*, 1766.
14. Nakamura, Y.; Adachi, M.; Kato, Y.; Fujii, S.; Sasaki, M.; Urahama, Y.; Sakurai, S. *J. Adhesion Sci. Technol.* **2011**, *25*, 869.
15. Nakamura, Y.; Adachi, M.; Ito, K.; Kato, Y.; Fujii, S.; Sasaki, M.; Urahama, Y.; Sakurai, S. *J. Appl. Polym. Sci.* **2011**, *120*, 2251.
16. Nakamura, Y.; Imamura, K.; Ito, K.; Nakano, S.; Sueoka, A.; Fujii, S.; Sasaki, M.; Urahama, Y. *J. Adhesion Sci. Technol.* **2012**, *26*, 231.
17. Nakamura, Y.; Sakai, Y.; Imamura, K.; Ito, K.; Fujii, S.; Urahama, Y. *J. Appl. Polym. Sci.* **2012**, *123*, 2883.
18. Hamada, K.; Morishita, Y.; Ishiura, K. Proceedings of The 30th Annual Meeting of The Adhesion Society, Tampa, FL, **2007**, p. 307.
19. Urahama, Y. *J. Adhesion Soc. Jpn.* **2010**, *46*, 53.
20. Ferry, J. D. *J. Am. Chem. Soc.* **1950**, *72*, 3746.
21. Dahlquist, C. A.; Hatfield, M. R. *J. Colloid Sci.* **1952**, *7*, 253.
22. Ferry, J. D. *Viscoelastic Properties of Polymers*, 3rd ed.; Wiley: New York, **1980**.
23. Fox, T. G. *Bull. Am. Phys. Soc. Ser. II* **1956**, *1*, 123.
24. Tse, M. F. *J. Adhesion Sci. Technol.* **1989**, *3*, 551.
25. Yang, H. W. H. *J. Appl. Polym. Sci.* **1989**, *55*, 645.